

Theoretical Investigation of Electronic Structures, Elastic, and Magnetic Properties of Rh₂CrGe Full-Heusler Alloy

M. MEBREK^{a,b,*}, A. MOKADDEM^{b,c}, F. BOUASRIA^d, B. DOUMI^{c,e}, A. MIR^f, A. YAKOUBI^a
AND A. BOUDALI^e

^aLaboratoire d'Etude des Matériaux et Instrumentations Optiques,
Département Matériaux et Développement Durable, Faculté des Sciences Exactes,
Université Djillali Liabes de Sidi Bel-Abbès, Sidi Bel-Abbès 22000, Algeria

^bCentre Universitaire Nour Bachir El Bayadh, El Bayadh 32000, Algeria

^cLaboratoire d'Instrumentation et Matériaux Avancés, Centre Universitaire Nour Bachir El-Bayadh,
BP 900 route Aflou, 32000 El Bayadh, Algeria

^dLaboratory of Knowledge Management and Complex Data,
Dr. Tahar Moulay University of Saida, 20000 Saida, Algeria

^eFaculty of Sciences, Department of Physics, Dr. Tahar Moulay University of Saida, 20000 Saida, Algeria

^fFaculty of Physics, Department of Science and Technology, Relizane University Centre, 48000 Relizane, Algeria

(Received March 2, 2019; revised version July 29, 2019; in final form August 2, 2019)

In this paper, we have investigated the structural, elastic, electronic, and magnetic properties of Rh₂CrGe full-Heusler alloy in the regular type (Cu₂MnAl, prototype *L*₂₁) phase by using the first-principle methods of density functional theory with local spin-density approximation. We have found that Rh₂CrGe is stable in the ferromagnetic configuration. This result is confirmed by the calculated cohesive energies. The stability criteria show that Rh₂CrGe is mechanically stable in *L*₂₁ structure. The spin-polarized electronic structures depicted a metallic character. The calculated total magnetic moment of 3.78 μ_B is not in agreement to the value of 4 μ_B of the Slater–Pauling rule. Therefore the Rh₂CrGe full-Heusler alloy is metallic ferromagnet in nature.

DOI: [10.12693/APhysPolA.136.454](https://doi.org/10.12693/APhysPolA.136.454)

PACS/topics: Rh₂CrGe, Heusler alloy, DFT, mechanical properties, electronic properties, magnetic moments

1. Introduction

The full and half-Heusler alloys have attracted important interest because of their potential applications as multifunctional materials for spintronic devices [1–3]. These compounds have important properties such as shape memory [4], superconducting, and thermoelectric materials [5, 6]. Among full-Heusler alloys there have been revealed a half-metallic feature [7–9]. Half-metallic Heusler alloys [10, 11] have been of great interest due to their ferromagnetic properties and half-metallic character with 100% spin polarization, implying that they are promising materials for exploitation in the spintronic applications [11–13]. The half-metallic ferromagnetic Heusler alloys are much more desirable than the other compounds for magneto-electronic applications [14, 15]. This is mainly due to the internal spin compensation generating additional advantages leading to a rather low value of the total magnetic moment in these alloys [15].

Several researchers have found that some full-Heusler alloys are not half-metals, but they exhibit a metallic character due to the metallic nature of their spin-polarized electronic structures [16–20]. The Rh₂FeAl [16]

and Fe₂NiZ (Z = Al, Ga, In) [17] full-Heusler alloys revealed metallic nature because the valence and the conduction bands dominate the Fermi level for two spins channels. However, Wei et al. [18] found that the metallic character of Fe₂NiTe alloy originates from the contribution of Fe- and Ni 3*d* states around the Fermi level. Although, Zhang et al. [19] and Wei [20] found that a pseudogap occurs below the Fermi level for minority-spin states and the Fermi level gradually moves from the shoulder of minority-spin states to the pseudogap [20].

The chemical formula of the Heusler alloys [21] is X₂YZ, where X and Y are transition elements and Z is a main group atom. The ordered full-Heusler cubic alloy X₂YZ crystallizes into two prototypical structures; the so-called “regular” type (Cu₂MnAl, prototype *L*₂₁) with space group *Fm* $\bar{3}$ *m* No. 225 and the Li₂AgSb type structure called “inverse” Heusler type with a space group *F* $\bar{4}$ 3*m* No. 216 (type Xa) [22]. For the *L*₂₁ prototype structure, the most electronegative element X occupies the position of the Wyckoff position 8c ($\frac{1}{4}, \frac{1}{4}, \frac{1}{4}$), Y is at 4b ($\frac{1}{2}, \frac{1}{2}, \frac{1}{2}$), and Z is at 4a (0, 0, 0) [11, 21, 22]. The X_a-type has four inequivalent positions in the unit cell, where the X₁ occupy 4d ($\frac{1}{4}, \frac{1}{4}, \frac{1}{4}$), Y in 4c ($\frac{3}{4}, \frac{3}{4}, \frac{3}{4}$), X₂ in 4b ($\frac{1}{2}, \frac{1}{2}, \frac{1}{2}$), and Z in 4a (0, 0, 0) [11, 21, 23].

The objective of this study is to investigate the structural, elastic, electronic, and magnetic properties of Rh₂CrGe compound. We have used the first-principle

*corresponding author; e-mail: mabrekoued22@gmail.com

methods of density functional theory [24, 25] within the local spin-density approximation (LSDA) [26] to determine the magnetic phase stability, elastic constants, the structural parameters, the spin-polarized electronic structures, and the ferromagnetic properties of Rh_2CrGe full-Heusler alloy. Our study is organized as follows: the computational method and the details of calculations are described in Sect. 2, the results are discussed in Sect. 3, and we end this work with a conclusion.

2. Computational method

We have performed the structural, electronic, and magnetic properties of Rh_2CrGe in the regular type (Cu_2MnAl , prototype $L2_1$) structure with space group $Fm\bar{3}m$ No. 225 as shown in Fig. 1 by using first-principle methods of density functional theory (DFT) [24, 25] based on the full-potential linearized augmented plane wave (FPLAPW) approach as implemented in WIEN2k code [27], where the exchange and correlation potential is treated by the local spin-density approximation (LSDA) of Perdew and Wang [26]. The cut-off energy is chosen as -0.6 Ry that determines the separation between the valence and the core states. The $R_{\text{MT}}K_{\text{max}}$ parameter was taken to be 7. To ensure the convergence of our calculations, we have taken $l_{\text{max}} = 10$. The used muffin-tin sphere radii are 2.0, 2.4, 1.95 a.u. (atomic unit) for Rh, Cr, and Ge atoms, respectively, in such a way that the muffin-tin spheres do not overlap. The charge density was Fourier expanded up to $G_{\text{max}} = 12$ (a.u.) $^{-1}$. In our calculations, the Rh [Kr]: $5s^14d^8$, Cr [Ar]: $4s^13d^5$, and Ge [Ar]: $4s^23d^{10}4p^2$ states are treated as valence states. The Monkhorst–Pack special k -point scheme with a 1500 special k -points in the Brillouin zone has been used for Rh_2CrGe alloy [28]. The self-consistent convergence of the total energy was set at 0.1 mRy.

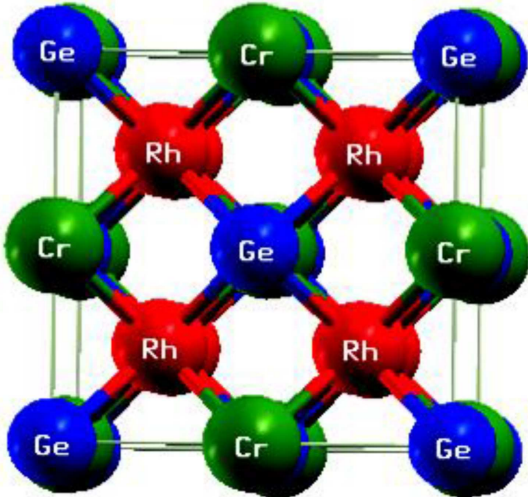


Fig. 1. The crystal structure of Rh_2CrGe alloy in the $L2_1$ phase.

3. Results and discussions

3.1. Structural properties

3.1.1. Magnetic stability and structural parameters

Firstly, we have determined the magnetic stability of the Rh_2CrGe compound by the calculated difference energy $\Delta E = E_{\text{NM}} - E_{\text{FM}}$ between the energies E_{NM} and E_{FM} of nonmagnetic (NM) and the ferromagnetic (FM) configurations, respectively. We have carried out the structural optimization by fitting the Murnaghan equation of state [29] that describes the variation of energies as a function of volumes as shown in Fig. 2. We have used in our calculations the predicted value of lattice parameter found by Gilleßen [30]. The obtained results such as equilibrium lattice constants (a), bulk modules (B), and their pressure derivatives (B'), and minimum total energies (E) of FM and NM configurations with other theoretical data [30, 31] are reported in Table I. We have found that the difference energy between the FM and NM states ΔE is equal to 0.054 eV. This positive value indicates that the FM state configuration of Rh_2CrGe is more stable than NM states.

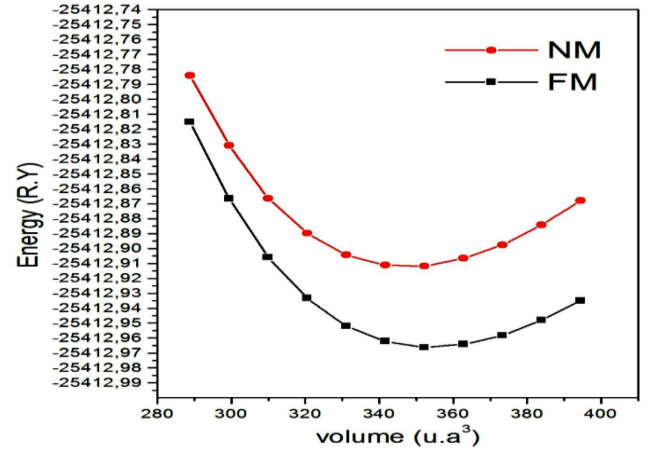


Fig. 2. The total energy as a function of unit cell volume of Rh_2CrGe alloy in ferromagnetic and non-magnetic configurations.

TABLE I

Calculated equilibrium lattice constants (a), bulk modules (B) and their pressure derivatives (B'), minimum total energies (E) and cohesive energies (E_{coh}) for Rh_2CrGe alloy.

Configuration	a [Å]	B [GPa]	B'	E [Ry]	E_{coh} [eV/atom]
ferromagnetic	5.94	242.08	4.79	-25412.965880	-7.75
non-magnetic	5.91	259.76	4.74	-25412.911983	-6.81
other calc.	6.091 [30]				
	5.57 [31]				

3.1.2. Cohesive energies

The cohesive energy reflects the stability of compound. In our case, we have characterized the stability of Rh_2CrGe compound in the ferromagnetic or

non-magnetic configurations by calculating the cohesive energies. The cohesive energy $E_{\text{coh}}^{\text{Rh}_2\text{CrGe}}$ is given by the following expression [32, 33]:

$$E_{\text{coh}}^{\text{Rh}_2\text{CrGe}} = \frac{[xE_{\text{atom}}^{\text{Rh}} + yE_{\text{atom}}^{\text{Cr}} + zE_{\text{atom}}^{\text{Ge}}] - E_{\text{total}}^{\text{Rh}_2\text{CrGe}}}{x + y + z}, \quad (1)$$

where x , y , and z are the numbers of Rh, Cr, and Ge atoms in the unit cell, respectively. The $E_{\text{total}}^{\text{Rh}_2\text{CrGe}}$ is the total energy of the unit cell, and the $E_{\text{atom}}^{\text{Rh}}$, $E_{\text{atom}}^{\text{Cr}}$, and $E_{\text{atom}}^{\text{Ge}}$ are the energies of the single Rh, Cr, and Ge atoms, respectively. The calculated values of the cohesive energies are summarized in Table I. The computed cohesive energies are 7.75, 6.81 eV/atom for FM and NM, respectively. Therefore, the larger absolute value of 7.75 eV means that the FM arrangement is more stable than that the NM state, which confirms the result obtained from the structural optimization.

3.1.3. Elastic properties and mechanical stability

The study of the elastic properties has an important role to know the nature of the bond between the neighbouring atomic planes, and the elastic constants describing the mechanical stability of the deformation of the crystalline face. It is the proportionality coefficients connecting the applied strain to the stress, which give the response of the material, its strength and mechanical stability under compression [12, 34, 35]. The computed elastic constants C_{11} , C_{12} , and C_{44} are summarized in Table II. From these parameters, it is possible to calculate the values of the mechanical stability criteria. In a cubic crystal, the mechanical stability is obtained when the following conditions are satisfied [36]:

$$\begin{aligned} C_{11} > 0, \quad C_{11}C_{12} > 0, \quad C_{44} > 0, \\ C_{11} + 2C_{12} > 0, \quad \text{and} \quad C_{12} < B < C_{11}. \end{aligned} \quad (2)$$

We have understood that the Rh₂CrGe compound is mechanically stable because our results verify the stability criteria [12, 36]. The C_{11} and C_{12} describe the response of the crystal to unidirectional compression, while C_{44} is proportional to the shear modulus and can be used as a measure of shear deformation. The value of C_{11} is larger than that of C_{44} of 586%. This reveals that Rh₂CrGe has more compressive strength than shear deformation. It can be seen from Table II that the calculated bulk modulus at zero pressure from elastic constants is 4% higher than that obtained by the total energy optimization. It gives an indication of the reliability and precision of our calculated elastic constants of Rh₂CrGe [12].

TABLE II

Calculated elastic constants for Rh₂CrGe alloy

Compound	C_{11} [GPa]	C_{12} [GPa]	C_{44} [GPa]
Rh ₂ CrGe	342.44	206.9	141.78

We have employed the Voigt–Reuss–Hill (VRH) approximation [37, 38] to calculate the bulk modulus (B) and the shear modulus (G) of Rh₂CrGe alloy given by $B = 1/3(C_{11} + 2C_{12})$ and $G = (C_{11}C_{12} + 3C_{44})/5$ expressions, respectively. The Young modulus (E) and the Poisson ratio (ν) of Rh₂CrGe alloy are computed respectively from the $E = 9BG/(3B + G)$ and $\nu = (3B - 2G)/2(3B + G)$ relations [37, 38]. The results of these parameters are given in Table III. The bulk modulus (B) determines the resistance of a material to volume change and reflects its response to a hydrostatic pressure. For cubic material, the shear modulus (G) is related to the second-order elastic constants [35]. The shear modulus (G) depicts the resistance of a material to shape change, while the Young modulus determines the resistance against uniaxial tensions. These parameters are important factors to define the mechanical features of a material [35]. We notice that there are no available data to compare with our results of elastic constants, bulk, and shear modulus. The calculated elastic constants are employed to calculate the Zener anisotropy parameter (A) [12, 37], which is given by the formula $A = 2C_{44}/(C_{11} - C_{12})$. It is an important physical feature that gives information on the degree of anisotropy in the solid structure. It can be said that if $A < 1$, the material is most rigid along the axis of the cube $\langle 100 \rangle$, whereas if $A > 1$ the material is most rigid along the diagonals of the body $\langle 111 \rangle$ [39]. We get the anisotropy parameter $A = 2.09$, and this value indicates that the Rh₂CrGe alloy is anisotropic. The anisotropy factor $A = 2.09 > 1$ reveals that Rh₂CrGe is more rigid along the diagonals of the body $\langle 111 \rangle$ in the $L2_1$ structure. From the criterion of Pugh [40] the B/G ratio is a ductility index of a material when it is larger than 1.75. In our case, the B/G ratio is 2.39, which means that the Rh₂CrGe compound is ductile.

TABLE III

Calculated bulk modulus B , shear modulus G , Young's modulus E , Poisson's ratio ν , criterion of Pugh B/G and anisotropic factor A for Rh₂CrGe alloy

Compound	E [GPa]	B [GPa]	G [GPa]	ν	B/G	A
Rh ₂ CrGe	272.73	252.07	105.43	0.316	2.39	2.09

3.2. Ferromagnetic properties and electronic structures

3.2.1. Magnetic moments

The calculated total and partial moments of Rh₂CrGe is given in Table IV. It shows that the main contribution of total magnetic moment is originated from the Cr atom. The ferromagnetic interaction results from the coupling between the positive magnetic moments of Cr and Rh atoms, while the antiferromagnetic coupling is produced between the positive magnetic moment of Cr atom and the negative magnetic moment of Ge. The calculated magnetic moment is in good agreement with theoretical calculation of Gilleßen [30].

TABLE IV

Calculated values of total and partial magnetic moments
Rh₂CrGe alloy

Compound	Total [μ_B]	Rh [μ_B]	Cr [μ_B]	Ge [μ_B]	Interstitial [μ_B]
Rh ₂ CrGe	3.78	0.32	2.69	-0.0014	0.46
other calculations	3.87 [30] 2.256 [31]				

We have compared the calculated total magnetic moment of Rh₂CrGe to the Slater–Pauling rule. This rule is used to calculate the total magnetic moment (M_t) of the Heusler alloys by the following formula $M_t = (Z_t - 24)$, where the Z_t is the valence electrons number per formula unit [16]. According to the Slater–Pauling rule, the total magnetic moment per unit cell M_t is $4 \mu_B$ for Rh₂CrGe alloy, whereas its total magnetic moment obtained by the LSDA approximation is $3.78 \mu_B$ (see Table IV). Therefore, the calculate total magnetic of $3.78 \mu_B$

is not in agreement with the Slater–Pauling rule because the conduction electrons at the Fermi level are not polarized fully [20]. Consequently, the Rh₂CrGe full-Heusler is metallic ferromagnet without half-metallic character. The metallic ferromagnetic behavior in Rh₂CrGe has been predicted in some full-Heusler alloys [17, 18, 20].

3.2.2. Band structures

We have calculated the band structures by the use of FPLAPW method with LSDA approximation. Figure 3 displays spin-polarized band structures of Rh₂CrGe compound along high symmetry direction in the first Brillouin zone. We have noticed that there is an overlap between the valence and conduction bands around Fermi level for both channels of spins, which is originated from the 3d (Cr) and 4d (Rh) bands that cross the Fermi level along the X-W directions. The band structures of both majority- and minority-spin bands show absence of band gap at the Fermi level, confirming the metallic nature of Rh₂CrGe alloy.

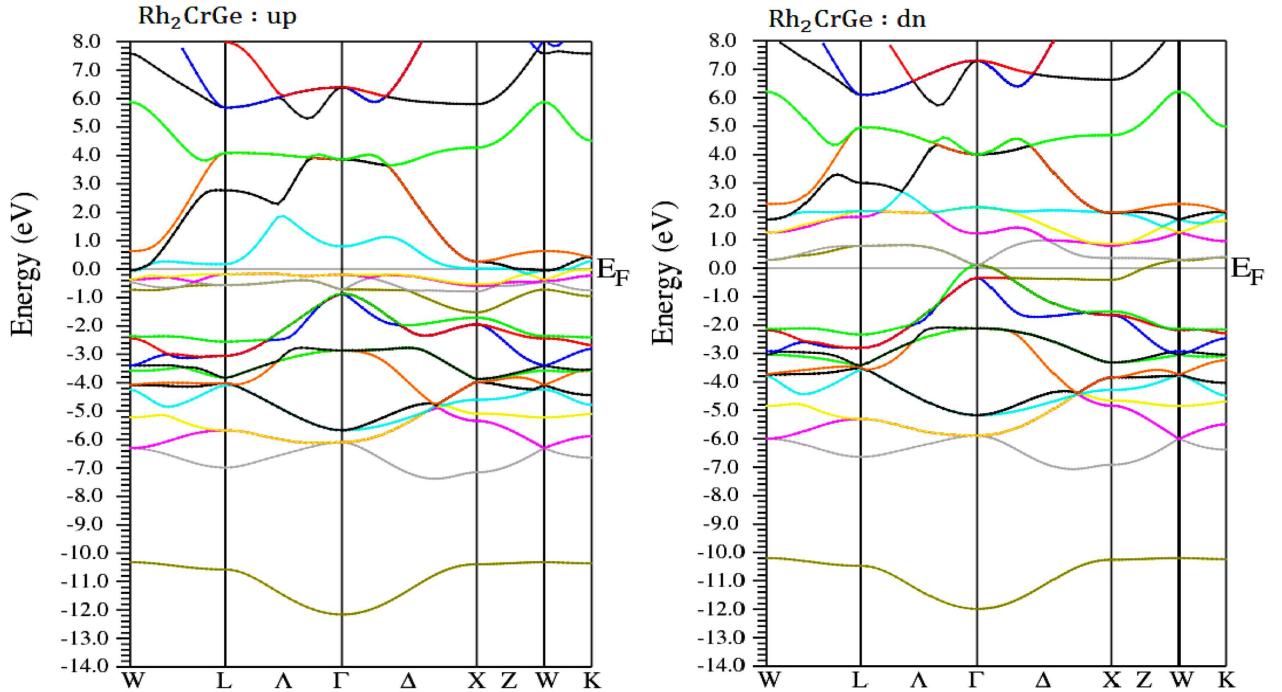


Fig. 3. The band structures of majority spin (up) and minority spin (dn) for Rh₂CrGe alloy.

3.2.3. Densities of states and charge densities

The calculated total and partial densities of states of Rh₂CrGe are shown in Fig. 4. It shows that the Fermi level is dominated by the densities of states for both spins directions and hence there is no gap at the Fermi level. Consequently, the Rh₂CrGe is metallic in nature. In addition, the total density of states of both majority- and minority-spin states depicted pseudo-gaps, which are situated below Fermi level. The metallic character around the Fermi level originates from the 3d (Cr) and 4d (Rh) states, while the contribution of the 4p (Ge) states

is almost absent. We understand that 3d (Cr) states mainly contribute in metallic nature compared to the 4d (Rh) states. To investigate the nature of chemical bonding in the Heusler alloys [17] we have performed the plot of charge density distribution along (110) plane Rh₂CrGe compound displayed by Fig. 5. It shows that amounts of charge are positioned between RhGe atoms and between CrGe. This means that electron accumulations between Rh–Ge is important compared to that between Cr–Ge, revealing that Rh–Ge and Cr–Ge have a common covalent bonding character.

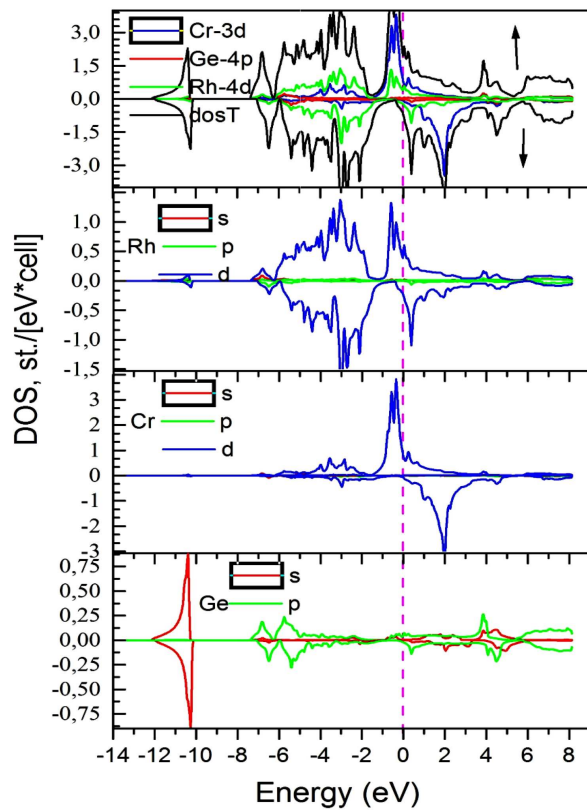


Fig. 4. Spin-polarized total and partial densities of states of majority spin (up) and minority spin (dn) for Rh_2CrGe alloy.

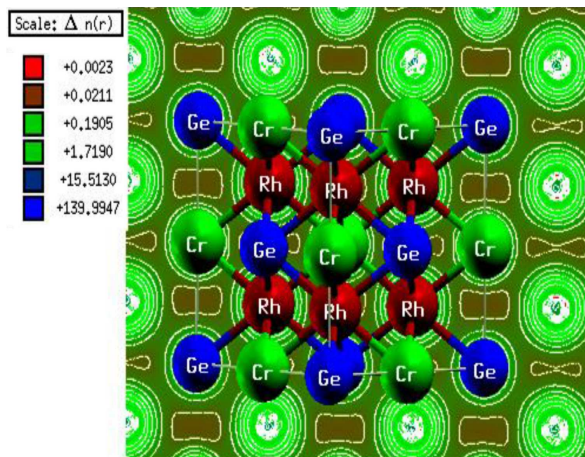


Fig. 5. Electronic charge densities of Rh_2CrGe alloy along (110) planes.

4. Conclusion

The first principle calculations of DFT within LSDA approximation were used to investigate the structural stability, elastic, electronic, and magnetic properties of Rh_2CrGe full-Heusler alloy in the regular type (Cu_2MnAl , prototype $L2_1$) phase. We have found that

the ferromagnetic configuration is stable compared to non-magnetic state. The stability in the ferromagnetic configuration is confirmed by the calculated cohesive energies. The mechanical stability criteria show that Rh_2CrGe compound is stable in the regular $L2_1$ structure. The origin of ferromagnetism in the Rh_2CrGe is mainly due to contribution of the 3d states of chromium (Cr). The calculated total magnetic moment of Rh_2CrGe is $3.78 \mu_B$, which does not respect the Slater–Pauling rule. The electronic structures for both spins directions revealed a metallic nature with pseudo-gap situated below the Fermi level. Therefore, results of electronic and magnetic properties suggest that the full-Heusler Rh_2CrGe alloy is metallic ferromagnet without half-metallicity.

References

- [1] H. Ohno, *Science* **281**, 951 (1998).
- [2] S.A. Wolf, D.D. Awschalom, R.A. Buhrman, J.M. Daughton, S. von Molnár, M.L. Roukes, A.Y. Chtchelkanova, D.M. Treger, *Science* **294**, 1488 (2001).
- [3] I. Žutić, J. Fabian, S. Das Sarma, *Rev. Mod. Phys.* **76**, 323 (2004).
- [4] Z.H. Liu, M. Zhang, Y.T. Cui, Y.Q. Zhou, W.H. Wang, G.H. Wu, X.X. Zhang, G. Xiao, *Appl. Phys.* **82**, 424, (2003).
- [5] T. Klimczuk, C.H. Wang, K. Gofryk, F. Ronning, J. Winterlik, G.H. Fecher, J.-C. Griveau, E. Colineau, C. Felser, J.D. Thompson, D.J. Safarik, R.J. Cava, *Phys. Rev. B* **85**, 174505 (2012).
- [6] J.W.G. Bos, R.A. Downie, *J. Phys. Condens. Matter* **26**, 433201 (2014).
- [7] C.G. Duan, R.F. Sabirianov, W.N. Mei, P.A. Dowben, S.S. Jaswal, E.Y. Tsymbal, *J. Phys. Condens. Matter* **19**, 315220 (2007).
- [8] X. Hu, *Adv. Mater.* **24**, 294 (2012).
- [9] S.E. Kulkova, S.V. Eremeev, T. Kakeshita, S.S. Kulkov, G.E. Rudenski, *Mater. Trans.* **47**, 599 (2006).
- [10] B.R.K. Nanda, I. Dasgupta, *J. Phys. Condens. Matter* **15**, 7307 (2003).
- [11] M. Chehroui, B. Doumi, A. Mokaddem, Y. Mogulkoc, M. Berber, A. Boudali, *J. Alloys Comp.* **722**, 564 (2017).
- [12] S. Wurmehl, G.H. Fecher, H.C. Kandpal, V. Ksenofontov, C. Felser, H.-J. Lin, J. Morais, *Phys. Rev. B* **72**, 184434 (2005).
- [13] I. Galanakis, P. Mavropoulos, P.H. Dederichs, *J. Phys. D Appl. Phys.* **39**, 765 (2006).
- [14] W.E. Pickett, J.S. Moodera, *Phys. Today* **54**, 39 (2001).
- [15] H. Zenasnia, H.I. Faraoun, C. Esling, *J. Magn. Magn. Mater.* **333**, 162 (2013).
- [16] S. Al, N. Arikan, S. Demir, A. Iyigör, *Physica B* **531**, 16 (2018).
- [17] D.C. Gupta, I.H. Bhat, *Mater. Chem. Phys.* **146**, 303 (2014).

- [18] X.P. Wei, X.W. Sun, T. Song, J.H. Tian, P. Guo, *J. Supercond. Novel Magn.* **31**, 2797 (2018).
- [19] H.G. Zhang, J. Chen, E.K. Liu, M. Yue, G.D. Liu, Q.M. Lu, W.H. Wang, G.H. Wu, *Intermetallics* **106**, 71 (2019).
- [20] X.P. Wei, Y.H. Zhou, *Intermetallics* **93**, 283 (2018).
- [21] J.L. Morán-López, R. Rodríguez-Alba, F. Aguilera-Granja, *J. Magn. Magn. Mater.* **131**, 417 (1994).
- [22] J.M. Khalaf Al-Zyadi, G.Y. Gao, K.L. Yao, *J. Alloys Comp.* **565**, 17 (2013).
- [23] L. Wollmann, S. Chadov, J. Kübler, C. Felser, *Phys. Rev. B* **90**, 214420 (2014).
- [24] P. Hohenberg, W. Kohn, *Phys. Rev.* **136**, B864 (1964).
- [25] W. Kohn, L.J. Sham, *Phys. Rev.* **140**, A1133 (1965).
- [26] J.P. Perdew, Y. Wang, *Phys. Rev. B* **45**, 13244 (1992).
- [27] P. Blaha, K. Schwarz, G.K.H. Madsen, D. Kvasnicka, J. Luitz, "WIEN2k, An Augmented Plane Wave Plus Local Orbital's, Program for Calculating Crystal Properties", Vienna University of Technology, Vienna 2001.
- [28] H.J. Monkhorst, J.D. Pack, *Phys. Rev. B* **13**, 5188 (1976).
- [29] F.D. Murnaghan, *Proc. Natl. Acad. Sci. U.S.A.* **30**, 244 (1944).
- [30] M. Gilleßen, Ph.D. Thesis, RWTH Aachen University, 2009.
- [31] W.H. Butler et al., *Heusler Database*, 2016.
- [32] A. Yakoubi, O. Baraka, B. Bouhafs, *Results Phys.* **2**, 58 (2012).
- [33] L. Fan, F. Chen, Z.Q. Chen, *J. Magn. Magn. Mater.* **478**, 264 (2019).
- [34] F.Z. Benkhalifa, A. Lekhal, S. Mécabih, *J. Supercond. Nov. Magn.* **26**, 2573 (2013).
- [35] S. Qi, C.H. Zhang, B. Chen, J. Shen, *Mod. Phys. Lett. B* **29**, 1550139 (2015).
- [36] J. Wang, S. Yip, S.R. Phillpot, D. Wolf, *Phys. Rev. Lett.* **71**, 4182 (1993).
- [37] A. Abada, K. Amara, S. Hiadsi, B. Amrani, *J. Magn. Magn. Mater.* **388**, 59 (2015).
- [38] Y. Benallou, K. Amara, B. Doumi, O. Arbouche, M. Zemouli, B. Bekki, A. Mokaddem, *J. Comput. Electron.* **16**, 1 (2017).
- [39] B.B. Karki, G.J. Ackland, J. Crain, *J. Phys. Condens. Matter* **9**, 8579 (1997).
- [40] S.F. Pugh, *Philos. Magn.* **45**, 823 (1954).